

Efficiency estimation of tray columns based on flow profiles and vapor-liquid equilibrium characteristics of binary mixtures

Vishwakarma, V.; Rigos, N.; Schubert, M.; Hampel, U.;

Originally published:

November 2019

Industrial & Engineering Chemistry Research 58(2019)51, 23347-23358

DOI: <https://doi.org/10.1021/acs.iecr.9b04915>

Perma-Link to Publication Repository of HZDR:

<https://www.hzdr.de/publications/Publ-29618>

Release of the secondary publication
on the basis of the German Copyright Law § 38 Section 4.

This document is confidential and is proprietary to the American Chemical Society and its authors. Do not copy or disclose without written permission. If you have received this item in error, notify the sender and delete all copies.

**Efficiency estimation of tray columns based on flow profiles
and vapor-liquid equilibrium characteristics of binary
mixtures**

Journal:	<i>Industrial & Engineering Chemistry Research</i>
Manuscript ID	ie-2019-04915d.R1
Manuscript Type:	Article
Date Submitted by the Author:	n/a
Complete List of Authors:	Vishwakarma, Vineet; Helmholtz-Zentrum Dresden-Rossendorf, Institute of Fluid Dynamics Rigos, Nireas; Helmholtz-Zentrum Dresden-Rossendorf, Institute of Fluid Dynamics Schubert, Markus; Helmholtz-Zentrum Dresden-Rossendorf, Institute of Fluid Dynamics Hampel, Uwe; Helmholtz-Zentrum Dresden-Rossendorf, Institute of Fluid Dynamics

SCHOLARONE™
Manuscripts

Efficiency estimation of tray columns based on flow profiles and vapor-liquid equilibrium characteristics of binary mixtures

Vineet Vishwakarma^{a,b,*}, Nireas Rigos^a, Markus Schubert^{a,*}, and Uwe Hampel^{a,b}

^aInstitute of Fluid Dynamics, Helmholtz-Zentrum Dresden-Rossendorf, Bautzner Landstraße 400,
01328 Dresden, Germany

^bChair of Imaging Techniques in Energy and Process Engineering, Technische Universität Dresden,
01062 Dresden, Germany

Abstract: A new systematic approach for estimating the section and column efficiencies based on flow profiles and vapor-liquid equilibrium (VLE) characteristics of binary mixtures exclusively for each tray is proposed. A novel iterative technique for approximating the slope of the VLE curve and the tray efficiency is also developed. For demonstrating the predictive capabilities of the new approach, two case studies are formulated in this work - one with a theoretical column processing selected binary mixtures at total reflux, and the other involving an industrial column whose performance data is acquired from the literature. An in-depth analysis of theoretical column study reveals the superiority of the new approach over the most applied method. In the case study of industrial column, the new approach predicts the section efficiency accurately, unlike the efficiency underestimation from the most applied method. Such an approach would allow a priori calculation of the section and column efficiencies in the tray and column design phase.

1. Introduction

Distillation is the leading separation technology in chemical process industries.¹ It is also likely to lead separations in the future mainly because of two reasons. First, it has distinct economic advantage while processing large throughputs.² Second, any alternative to this industrially viable technique is not yet available.^{1,3} A recent estimate in 2016 claims that column distillation accounts for 10 to 15% of the global energy consumption.⁴ These columns also demand up to 50% of both capital and operational costs in industrial processes.⁵ Half of the columns existing worldwide are equipped with cross-flow trays, and this trend is also likely to continue in the future.⁶ Among these columns, the most common internals are the single-pass cross-flow trays.⁶ In fact, such columns are viewed as cascades of trays with similar geometries and functions.³ This generalized perspective has prompted numerous experimental and theoretical studies on hydrodynamics and mass transfer efficiency of individual trays. The majority of the existing studies covered the hydrodynamic aspects of sieve trays such as flow capacity, pressure drop, holdup distribution, weeping and so forth.¹ It is known that the tray hydrodynamics are affected by flow maldistribution. However, only few studies investigated the two-phase flow and mixing patterns on these trays through experiments and CFD simulations. Even fewer proposed models for associating these patterns with the Murphree tray efficiency. Such models are based on relationships developed from the analyses of two-phase flow, cross-flow hydraulics and mass transfer over the trays.⁷ A collective description of the aforesaid experimental and theoretical studies can be found in the literature.^{1,3}

Thousands of columns operating worldwide suggest that any improvement in distillation technology could potentially reduce their cost and energy expenditures on a global scale.^{1,8} But, to quantify any progress, methods for estimating the overall column efficiency should be at hand. As already mentioned, the prediction of the tray efficiency based on flow and mixing profiles over a single column tray is possible. However, adequate utilization of the individual tray efficiencies in the column efficiency estimation has not been attempted in the literature. In other words, the existing

1
2
3 approaches for the column efficiency prediction do not exclusively consider the individual tray
4 efficiencies governed by flow and mixing profiles and vapor-liquid equilibrium (VLE) characteristics
5 of the mixtures. For supporting the previous assertions, the existing approaches are briefly revisited
6 here. The definition of the overall tray column efficiency is
7
8
9
10

$$E_o = \frac{N_{eq}}{N} \quad , \quad (1)$$

11
12
13
14
15
16 where N_{eq} is the number of equilibrium stages (obtained using the McCabe-Thiele (MT) method),⁹
17 and N is the actual number of trays in the column.³ Usually, eq 1 is used for estimating section
18 efficiencies in a column in case there are two or more sections owing to feed and side draw streams.
19
20
21 It is allowed to use eq 1 for determining the overall column efficiency, if the whole column is
22 considered as one section.¹ The simplest method for estimating the column efficiency is the
23 O'Connell's correlation,^{10,11} which is
24
25
26
27
28
29

$$E_o = 0.503(\mu_L \cdot \alpha_{avg})^{-0.226} \quad . \quad (2)$$

30
31
32 Here, α_{avg} is the average relative volatility of a binary mixture, and μ_L is the liquid viscosity of the
33 feed (in mPa·s), both calculated at the average column temperature. This equation is known to
34 provide conservative estimations that are suitable for preliminary studies only,¹ and to ignore the
35 explicit inclusion of parameters representing the mass-transfer performance.¹¹ Further, in this
36 correlation, the reason for including the relative volatility over more relevant parameters such as
37 the slope of the VLE line (m) or the stripping factor ($\lambda (= mV/L)$) is also unclear.^{1,11} In another
38 study, Lewis¹² forecasted the impact of the tray efficiency on the overall column efficiency as
39
40
41
42
43
44
45
46
47

$$E_o = \frac{\ln \{1 + E_{MV}(\lambda - 1)\}}{\ln \lambda} \quad . \quad (3)$$

48
49
50
51
52 In eq 3, it is assumed that the VLE and the operating lines are straight but may not be necessarily
53 parallel along with a constant tray efficiency for each tray.¹ This equation has found application in
54
55
56
57

1
2
3 the renowned AIChE's bubble-tray design manual.¹³ In reality, the stripping factor varies over a
4 column because of the variation of the VLE data and the slope of the operating lines. The stripping
5 factor and the tray efficiency have been assumed as constant over the whole column in eq 3, thus,
6 rendering this method acceptable only for approximate estimations. Recently, Mathias¹⁴ calculated
7 the actual number of trays in a column by resorting to a graphical technique similar to the MT
8 method. In that study, a stepping procedure was followed between VLE and operating lines on an x -
9 y chart based on a fixed tray efficiency, unlike the MT method, where the same procedure is applied
10 for the equilibrium trays (i.e., trays with 100% Murphree efficiency). Assigning a fixed efficiency to
11 each tray for the column efficiency calculation suggests the applicability of this approach for
12 qualitative evaluations only.¹⁴ Further, Górak and Schoenmakers² suggested the capacity and
13 efficiency testing of trays during their development stage for identifying potential design problems
14 and subsequent improvements. Schultes¹⁵ confirmed that such practice is non-existent for new
15 trays and emphasized the need for pre-emptive calculations of fluid dynamics and separation
16 efficiency during their development phase. In addition, Taylor¹⁶ acknowledged the necessity of
17 approaches for calculating thermodynamic properties needed in the efficiency models and for
18 modeling the performance of distillation columns. Therefore, a methodical approach is needed for a
19 priori estimation of the section and column efficiencies based on tray-to-tray efficiency calculations
20 governed by flow and mixing profiles and VLE characteristics of the mixtures. Instead, potential
21 areas for improving tray and hence, column performances are currently identified in the post-
22 design phase leading to considerable losses in the industry.¹⁵

23
24
25
26
27
28
29
30
31
32
33
34
35
36
37
38
39
40
41
42
43
44
45
46
47
48
49
50
51
52
53
54
55
56
57
58
59
60
The objective of this work is to formalize a new systematic strategy for evaluating the section and
column efficiencies involving flow and mixing profiles on single-pass cross-flow trays and VLE data
of binary mixtures. At first, appropriate thermodynamic models are employed for generating the
VLE data of the binary mixtures. Liquid flow profiles in the form of residence time distributions
(RTD) are assigned to the trays using the axial-dispersion model (ADM). Further, vapor plug flow is

1
2
3 considered through the trays with perfect mixing occurring in the disengagement zones between
4 them. A novel iterative approach is then proposed that considers these information, and computes
5 the slope of the VLE line and the tray efficiency using the standard tray efficiency model. Following
6 the new approach for tray-to-tray efficiency calculations allows obtaining the resultant column
7 efficiency. Two case studies are presented in this work to elucidate the proposed strategy. In the
8 first study, a theoretical column operating at total reflux is considered for selected binary mixtures.
9 In the second study, the same approach is employed for examining real column data acquired from
10 the literature.
11
12
13
14
15
16
17
18
19
20
21
22

23 **2. Case study I**

24 **2.1 Column configuration, test systems and VLE data**

25
26
27 In the literature, the overall column efficiency is usually monitored for tray columns operating at
28 total reflux (see Figure 1a).^{2,13,17,18} In such configuration, all vapor leaving through the column top is
29 fully condensed and routed back to the column as reflux. Further, all liquid leaving through the
30 bottom of the column is vaporized in the reboiler and returned back to the column.² This leads to
31 equality between the liquid and vapor molar flow rates (i.e., $L = V$). Such equality is advantageous
32 for estimating the column performance, which is sensitive to the L/V ratio. According to Lockett,¹
33 inaccuracies in the measured reflux ratio can cause significant errors in the efficiency calculations.
34 The absence of feed and product streams in this configuration further avoids possible feed
35 fluctuations and discrepancies between the feed inlet and feed-tray compositions.¹⁹ On the other
36 hand, the studies with finite reflux are scarce and usually preferred for hydraulic studies only.²
37
38
39
40
41
42
43
44
45
46
47
48
49
50
51
52
53
54
55
56
57
58
59
60

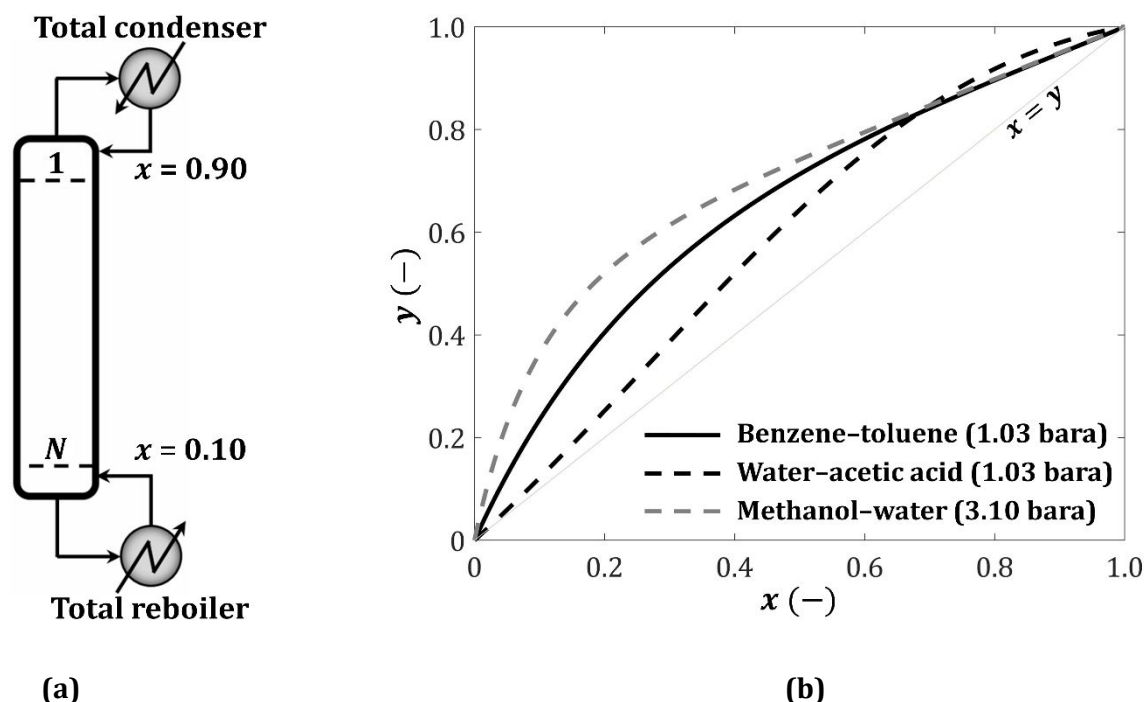


Figure 1. (a) Tray column operating at total reflux mode and (b) VLE plot of standard binary mixtures at given total pressures.

Accurate VLE data are the prerequisites for column performance simulations.^{1,2} According to Kister,¹⁸ any uncertainty in such data results in inaccurate tray-to-tray efficiency calculations, particularly for low volatility systems. Many different thermodynamic models exist in the literature for generating physical and thermodynamic properties of the processes, such as Soave-Redlich-Kwong (SRK), Non-Random Two-Liquid (NRTL), Hayden-O'Connell (HOC), Peng-Robinson (PR), Universal Quasichemical (UNIQUAC), and so forth.¹⁵ Recently, De Hemptinne and Ledanois²⁰ reported a list of criteria (i.e., decision tree) for an appropriate selection of thermodynamic models for industrial applications. Seader et. al¹⁹ also reported a list of industrial binary distillation operations with representative values of the total column pressure. From this literature, the test systems and their representative pressures are derived. Suitable thermodynamic models are selected for these systems based on the earlier mentioned decision tree²⁰ and other references.^{21,22}

Table 1¹⁹ summarizes the selected binary mixtures, column pressures and applied thermodynamic models.

Table 1. Binary mixtures with representative column pressures, thermodynamic models, relative volatilities and minimum number of trays in the column.

Binary mixture	Operating pressure (bara)	Thermodynamic model	α_{avg} (-)	N_{min} (-)
Propylene-propane	19.31	Soave-Redlich-Kwong (SRK) ²⁰	1.12	37.21
m-xylene-o-xylene	1.03	Soave-Redlich-Kwong (SRK) ²⁰	1.14	32.58
Vinyl acetate-ethyl acetate	1.03	Non-Random Two-Liquid (NRTL) ²⁰	1.16	29.43
Isopentane-n-pentane	2.07	Soave-Redlich-Kwong (SRK) ²⁰	1.26	19.06
Isobutane-n-butane	6.90	Soave-Redlich-Kwong (SRK) ²⁰	1.30	17.00
Ethylene-ethane	15.86	Soave-Redlich-Kwong (SRK) ²⁰	1.54	10.19
Methanol-ethanol	1.03	Universal Quasichemical (UNIQUAC) ²⁰	1.68	7.94
Acetic acid-acetic anhydride	1.03	Non-Random Two-Liquid (NRTL) - Hayden-O'Connell (HOC) ²¹	1.73	14.48
Toluene-ethylbenzene	1.03	Soave-Redlich-Kwong (SRK) ²⁰	1.98	6.54
Water-acetic acid	1.03	Non-random two-liquid (NRTL) - Hayden-O'Connell (HOC) ²¹	2.08	9.91
Benzene-toluene	1.03	Soave-Redlich-Kwong (SRK) ²⁰	2.37	4.88
Propane-1,3-butadiene	8.27	Soave-Redlich-Kwong (SRK) ²⁰	2.58	4.73
Methanol-water	3.10	Cubic-Plus-Association (CPA) ²²	3.27	3.89
Cumene-phenol	0.07	Universal Quasichemical (UNIQUAC) ²⁰	4.21	2.75
Benzene-ethylbenzene	1.03	Soave-Redlich-Kwong (SRK) ²⁰	4.87	2.90

The VLE data for the test systems were acquired from the large built-in database of Aspen Plus (v10) based on column pressure, thermodynamic model and number of data points (i.e. resolution) needed. Mathias¹⁴ recommended a large number of data points for complex VLE diagrams; hence, 500 data points are generated for every mixture. The VLE diagrams of three of the mixtures listed in

1
2
3 Table 1 are illustrated in Figure 1b. In this figure, a distinction in the equilibrium characteristics of
4 these mixtures is visible, which is important for understanding their influence on the overall column
5 efficiency. The compositions of the more volatile component in condenser and reboiler streams
6 (refer to Figure 1a) are maintained at 90% and 10%, respectively. This is based on the
7 recommendation of Górak and Schoenmakers,² since extreme component purities in these streams
8 may lead to errors in the VLE data analyses. It should be noted that the mixtures in Table 1 are
9 arranged in the ascending order of α_{avg} , which is the average relative volatility of the light
10 component relative to the heavy component. In the nomenclature of binary mixtures, the first
11 compound is the light component, e.g., methanol is the more volatile component in the methanol-
12 water mixture. Besides, the relative volatility (α) between the components is generally uniform over
13 the entire column for hydrocarbon mixtures, whereas for aqueous systems, alcohol mixtures and
14 other systems, α varies considerably over the column. In any case, the relative volatility is averaged
15 over the column as

$$\alpha_{avg} = \sqrt{\alpha_T \alpha_B} \quad , \quad (4)$$

16
17
18
19
20
21
22
23
24
25
26
27
28
29
30
31
32
33
34
35 where α_T and α_B represent the relative volatilities of the streams leaving top and bottom of the
36 column, respectively. Further, Lockett¹ and Kister¹⁸ suggested to provide VLE data along with
37 efficiency calculations. Thus, reduced VLE data (i.e. with 50 points) for each mixture are provided in
38 Table S1 in the Supplementary Information. All 500 VLE data points for these mixtures are
39 accessible in the RODARE repository.²³ In addition, Table 1 also mentions the minimum number of
40 stages (N_{min}) needed in the column for each mixture based on the prescribed specifications of the
41 condenser and reboiler streams. In fact, N_{min} also specifies the equilibrium number of stages in the
42 column at total reflux, which can be calculated using the renowned Fenske's equation. However,
43 Górak and Sorensen⁵ reported that this equation is unreliable, when α varies noticeably over the
44 column. Thus, these stages are obtained using the MT method applied in MATLAB (R2017b) as
45 shown in Figure S1 in the Supplementary Information. In addition, Górak and Olujić⁶ emphasized

1
2
3 the need of conservative approaches for estimating the column efficiency. Schultes¹⁵ also agreed on
4 the inclusion of safety margins in the column design, especially where information or experience
5 pertaining to column design is incomplete or missing. Hence, the fractional number of equilibrium
6 stages, as given in the Table 1, and actual number of trays rounded off to the next integer will be
7 considered in eq 1 for conservative predictions of the column efficiencies.
8
9
10
11
12
13
14
15
16

17 **2.2 Flow description on column trays**

18
19 The description of the two-phase flow in a column is essential for its performance calculation.
20 Basically, the information about the flow over one column tray would be sufficient, if the tray
21 column is considered as a stack of trays that are geometrically and functionally similar.³ Several
22 studies in the literature claim that flow and mixing patterns of the individual phases have strong
23 influence on the mass transfer characteristics of trays.³ Plug flow is considered ideal for the tray
24 performance.¹² Sahai and Emi²⁴ stated that mixing in the axial (i.e., flow-wise) direction is non-
25 existent at plug flow, however, there may be mixing in the transverse direction (i.e., orthogonal to
26 the main flow direction) to any extent. Shah et al.²⁴ supported this definition of plug flow only for
27 complete mixing in the transverse direction. Any deviation from plug flow, referred to as non-ideal
28 flow or flow maldistribution, is considered detrimental to the tray efficiency.²⁵ This holds for both
29 liquid and vapor flow over the tray.²⁶ As observed in experimental studies reported in the
30 literature,³ liquid flow is represented by the residence time distribution (RTD) here, while
31 presuming vapor plug flow through the trays. The RTD is a well-known concept in chemical
32 engineering that is used for analyzing the flow behavior in continuous flow systems.²⁷ According to
33 this concept, the fluid elements follow different routes in a system, and thus, require different times
34 to leave it. The distribution of these times for the fluid elements leaving the system is represented
35 by the RTD function ($f(t)$). For instance, the RTD functions for a plug flow reactor and an ideal
36
37
38
39
40
41
42
43
44
45
46
47
48
49
50
51
52
53
54
55
56
57
58
59
60

continuous stirred-tank reactor are $\delta(t - \tau)$ and $\tau^{-1}e^{-t/\tau}$, respectively. Here, τ is the mean residence time of the fluid elements defined as

$$\tau = \int_0^{\infty} tf(t)dt \quad . \quad (5)$$

An in-depth coverage of the RTD concept and the techniques for determining the RTD functions of systems can be found elsewhere.^{28,29} Different models are used for describing the flow behavior (i.e., macromixing characteristics) in continuous flow systems, such as the axial dispersion model (ADM) and the tanks-in-series model (TISM), to name a few.³⁰ According to Levenspiel,²⁸ both these models are approximately equivalent to each other, but the physical basis of the TISM is not as clear as that of the ADM. The former describes the RTD in terms of integral number of ideal CSTRs only.³¹ The analytical solution of the ADM for the open-open boundary condition provides the RTD function that is often preferred in the experiments²⁸ as

$$f(t) = \frac{1}{\sqrt{4\pi t\tau_h N_{TD}}} \cdot \exp\left\{-\frac{(1 - t/\tau_h)^2}{4tN_{TD}/\tau_h}\right\} \quad . \quad (6)$$

Here, τ_h is the hydraulic time that is based on bulk liquid velocity and flow path length (Z) of the tray. Further, N_{TD} is the dimensionless parameter referred to as tray dispersion number²⁵ that is defined as

$$N_{TD} = \frac{D_E \cdot \tau_h}{Z^2} \quad . \quad (7)$$

The reciprocal of the tray dispersion number is called Péclet number (Pe). In eq 7, D_E is the axial dispersion coefficient that characterizes liquid backmixing in a system.²⁵ Hence, higher dispersion number means higher liquid mixing in the axial direction on the tray, and vice-versa.²⁵ Based on these information, three different arbitrary RTD functions (Cases I to III) are prescribed to the liquid flow on the trays (by assuming dispersion numbers and hydraulic times in eq 6) as shown in Figure

2. This figure is presented with a limited time scale (i.e., up to 60 s) for better illustration of these functions. From Case I towards Case III, the dispersion number or the amount of axial liquid mixing on the tray is decreasing. The higher the axial liquid mixing on the tray, the higher the tray efficiency loss.²⁵ Therefore, the tray efficiency for constant point efficiency (E_{OV}) and stripping factor over the tray should be the lowest in Case I, intermediate in Case II, and the highest in Case III. This behavior will be inspected in detail in the upcoming sections.

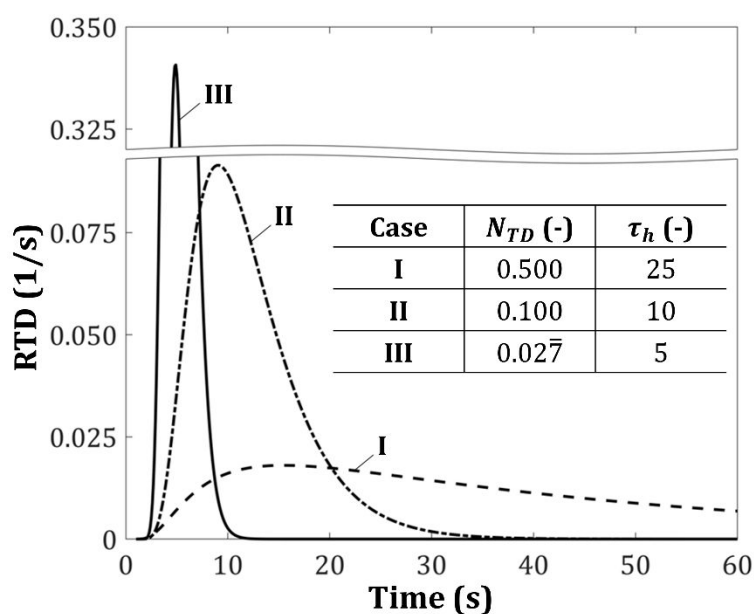


Figure 2. RTD functions and associated parameters of the three cases.

2.3 Tray-to-tray efficiency calculations

Kister et al.³² proposed a sequence of steps for converting individual phase resistances into column efficiency via Lewis¹² definition (eq 3) using information such as stripping factor, flow distribution, entrainment and weeping. Basically, this procedure assumes one tray as a representative for a section or the whole column, and estimates the section or column efficiency based on the selected tray conditions.¹ A similar approach is used here, as shown in Figure 3, except that tray-to-tray

efficiency calculations are preferred over eq 3. This allows to incorporate variations in hydraulic conditions, thermodynamic equilibrium, design characteristics and so forth, in the overall efficiency estimation.

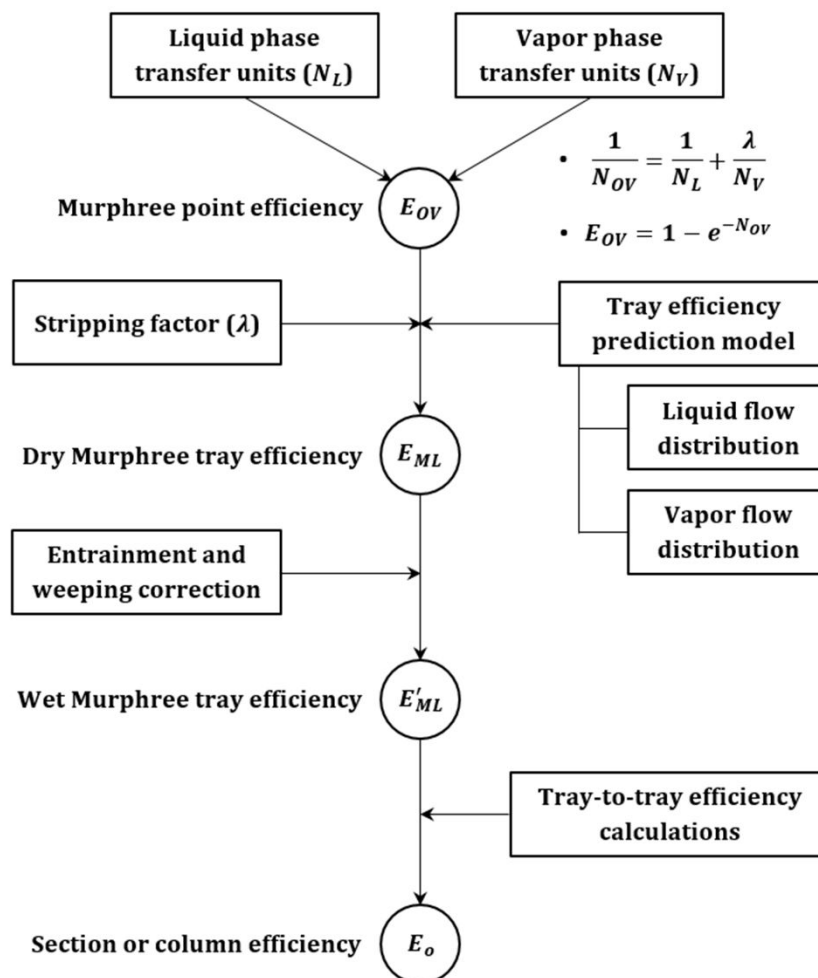


Figure 3. Sequence of steps for the section or column efficiency prediction.

Firstly, the vapor and liquid phase transfer units (referred to as N_V and N_L , respectively) are estimated based on the two-film resistance theory. The phase resistances are then added up to get the overall vapor phase transfer units (N_{OV}), from which the Murphree vapor-side point efficiency (E_{OV}) is estimated using an appropriate literature model.^{1,32} Based on AIChE's bubble-tray design manual,¹³ several studies have considered distillation to be a vapor-phase-controlled (i.e., negligible

liquid-phase resistance) operation.³³ However, experimental data in the literature^{1,34-37} indicate that the liquid-phase resistance can also be significant.³³ To acknowledge these facts, the transfer units of the individual phases on the tray are considered as equal, i.e., $N_V = N_L$. This is applied to all trays in the column. No numerical values are prescribed to these units, since they require an individual description of mass-transfer coefficients, interfacial area, and residence times according to Lockett.¹ Instead, the point efficiency (E_{OV}) is considered to be constant on each tray in the column for the given equality. Two arbitrary cases of E_{OV} as 30% and 60% are considered here. This would further allow understanding their effect on the overall column efficiency. Then, a mathematical model is needed for converting the point efficiency into tray efficiency based on flow and mixing patterns of the individual phases and the VLE data.³² Different tray efficiency prediction models are available in the literature, namely plug flow model,¹² pool models,³⁸⁻⁴⁰ diffusional models,⁴¹⁻⁴³ non-uniform flow model,⁴⁴ RTD model,⁴⁵ and others.^{25,26} The RTD model is selected here, because it accounts for all possible types of liquid flow behavior on a tray and thus, provides the most realistic estimation of the tray efficiency. According to this model, the Murphree vapor-phase and liquid-phase tray efficiencies are

$$E_{MV} = \frac{1 - \int_0^{\infty} e^{-\lambda E_{OV} t / \tau} \cdot f(t) dt}{\lambda \int_0^{\infty} e^{-\lambda E_{OV} t / \tau} \cdot f(t) dt}, \text{ and} \quad (8)$$

$$E_{ML} = \frac{1 - \int_0^{\infty} e^{-\lambda E_{OV} t / \tau} \cdot f(t) dt}{1 - \frac{1}{\lambda} \left\{ 1 - \int_0^{\infty} e^{-\lambda E_{OV} t / \tau} \cdot f(t) dt \right\}}, \quad (9)$$

respectively. Foss⁴⁶ validated this model through oxygen-stripping studies on a rectangular sieve tray operated with oxygen-rich water and air. Detailed information regarding this model, especially its mathematical formulation, associated assumptions and experimental validation, can be found elsewhere.^{3,25,45,46} Three RTD functions (Cases I to III) representing the liquid flow on the column trays are already defined (see Section 2.2) for the model application. The mean residence time for

each case can be calculated using eq 5. In addition, plug flow of vapor through the trays and perfect mixing in the disengagement zones between them are assumed in this model. Recently, new tray concepts⁴⁷⁻⁵⁰ have demonstrated reasonably uniform vapor distribution, and hence, the standard efficiency prediction models are directly applicable to those trays. Besides, based on the assumption of linear VLE relationship (for an expected composition range over a tray) and the total reflux operation, λ for a tray reduces to the slope (m) of the VLE line.

As per authors' knowledge, the only known approach for calculating m can be found in AIChE's design manual.¹³ That approach was proposed for VLE data with large curvature only, and by assuming that liquid on the tray is perfectly mixed. This implies that the tray and point efficiencies are the same for the tray (e.g., $E_{MV} = E_{OV}$),³ while E_{MV} is usually greater than E_{OV} due to imperfect (or partial) liquid mixing on the tray.¹ Hence, a more general approach that is devoid of the limitations stated above is explained in Figure 4. This figure is provided for illustration only and does not depict any particular case of column simulation. For better understanding of the explanations below, the top-to-bottom approach is applied for labelling the trays as well as for the efficiency calculations.⁵ According to Lockett,¹ E_{MV} and E_{ML} should be preferred when moving up and down in the column, respectively. In this study, eq 9 and the common definition of E_{ML} , i.e.,

$$E_{ML} = \frac{x_n - x_{n-1}}{x_n^* - x_{n-1}} \quad , \quad (10)$$

for the n^{th} tray is used. In eq 10, x_{n-1} and x_n are the average compositions of the liquid stream entering and leaving the n^{th} tray, respectively, and x_n^* is the liquid composition that is in equilibrium with the composition of vapor exiting that tray. According to eqs 9 and 10, an accurate determination of λ (or m) is essential for correct values of E_{ML} and x_n .

For any given x_{n-1} (i.e., the composition of the reflux liquid at column top here), the corresponding x_n^* can be obtained using the MT method as shown in Figure 4a. The nomenclature of each line used in Figure 4 is also provided there. In the new approach, m is initially assumed for the tray, and the

1
2
3 resulting E_{ML} and x_n are calculated using eqs 9 and 10, respectively. These parameters are then
4
5 iterated collectively and progressively until the variations in each of their successive numerical
6
7 values are less than 10^{-4} . For doing so, it is crucial to identify the range of the VLE data that needs to
8
9 be considered for the slope calculation specific to a tray. Such range depends on the transfer units
10
11 and the molar flow rates of the two phases as suggested in AIChE's manual.¹³ For this purpose, the
12
13 supporting lines are drawn with the slope $\beta = (-N_L \cdot L)/(N_V \cdot V)$ from x_n^* and x_{n-1} on the diagonal
14
15 line. Since $N_L = N_V$ and $L = V$, the slope of these lines is 135° as shown in in Figure 4b. In the same
16
17 figure, the supporting lines intersect the VLE curve at points i^* and j , respectively. Between i^* and j
18
19 , the VLE curve is fitted (in the least-squares sense) with a straight line using the 'polyfit' function in
20
21 MATLAB (refer to Figure 4c). The slope of the fitted line is the initial estimate called m^* there. As
22
23 given in Remark 1 in Figure 4, m^* is then supplied to eq 9 for calculating E_{ML} . From this E_{ML} , the
24
25 first estimate of x_n , referred to as x_n^1 , is obtained using eq 10 (see Figure 4d). Since x_{n-1} is fixed for
26
27 the tray, the location of point j on the VLE curve remains unchanged throughout in Figure 4. Now,
28
29 the supporting line with the slope β is drawn from point x_n^1 on the diagonal line intersecting the VLE
30
31 curve at i^1 as shown in Figure 4d. Then, the VLE curve between i^1 and j is fitted with a straight line,
32
33 as explained earlier, to obtain the new estimate of m (referred to as m^1 in Figure 4e). According to
34
35 Remark 2 in Figure 4, the new value of x_n (called x_n^2) is estimated as shown in Figure 4f. The
36
37 procedure discussed so far is repeated (e.g., k times in Figure 4g) until the difference in the
38
39 consecutive numerical values of each m , E_{ML} and x_n is below 10^{-4} . Not more than 10 iterations were
40
41 required to satisfy the prescribed criteria. Eventually, the correct values of m ($= m^k$, not shown
42
43 here), E_{ML} , i^k , and x_n ($= x_n^k$) are obtained as shown in Figure 4g. Here, point i^k represents liquid and
44
45 vapor compositions at the interface, where the vapor enters the tray. Similarly, point j represents
46
47 these compositions at the interface, where the vapor leaves the tray.¹³ Furthermore, it is assumed
48
49 that there is no entrainment and weeping, which leads to $E_{ML} = E'_{ML}$ in Figure 3. So, the estimated
50
51 composition of the liquid stream exiting the n^{th} tray becomes the inlet composition for the next tray.
52
53
54
55
56
57

1
2
3 This was considered in the graphical study of Mathias,¹⁴ which can happen because of perfect liquid
4 mixing in the downcomer. This entire procedure involving eqs 9 and 10, and Figures 3 and 4 is
5 repeated for the next tray and so forth, until the actual tray step reaches the composition of the
6 liquid leaving the column at the bottom, which is 0.1. This way, the efficiency of each tray, and
7 hence, the actual number of trays in the column are calculated. The readers are referred to Lockett,¹
8 Kister et al.³² and Foss⁴⁶ for the assumptions (not given here) involved in the mentioned steps in
9 Figure 3.
10
11
12
13
14
15
16
17

18 An alternate approach to the line fitting method proposed above is the averaging of the slope of the
19 VLE curve over the required range. Such an approach can also be used for the slope estimation in
20 Figures 4c, 4e and others. For instance, the VLE curve between points i^k and j in Figure 4g is firstly
21 fitted with a second degree univariate polynomial (i.e., $y(x) = ax^2 + bx + c$) using the 'polyfit'
22 function in MATLAB. Here, a, b and c are the coefficients of this polynomial with $a \neq 0$. Thus,
23 calculating the derivative of this quadratic function (i.e., $y'(x) = 2ax + b$) at each abscissa point
24 between points i^k and j and averaging the resulting y' values provides m for the tray. Both
25 approaches are equivalent and produce identical values of m for each column tray. This is
26 exemplarily shown for the binary systems water-acetic acid, benzene-toluene, and methanol-water
27 in Table S2 in the Supplementary Information.
28
29
30
31
32
33
34
35
36
37
38
39
40
41
42

43 **Space left for Figure 4**
44
45
46
47
48
49
50
51
52
53
54
55
56
57

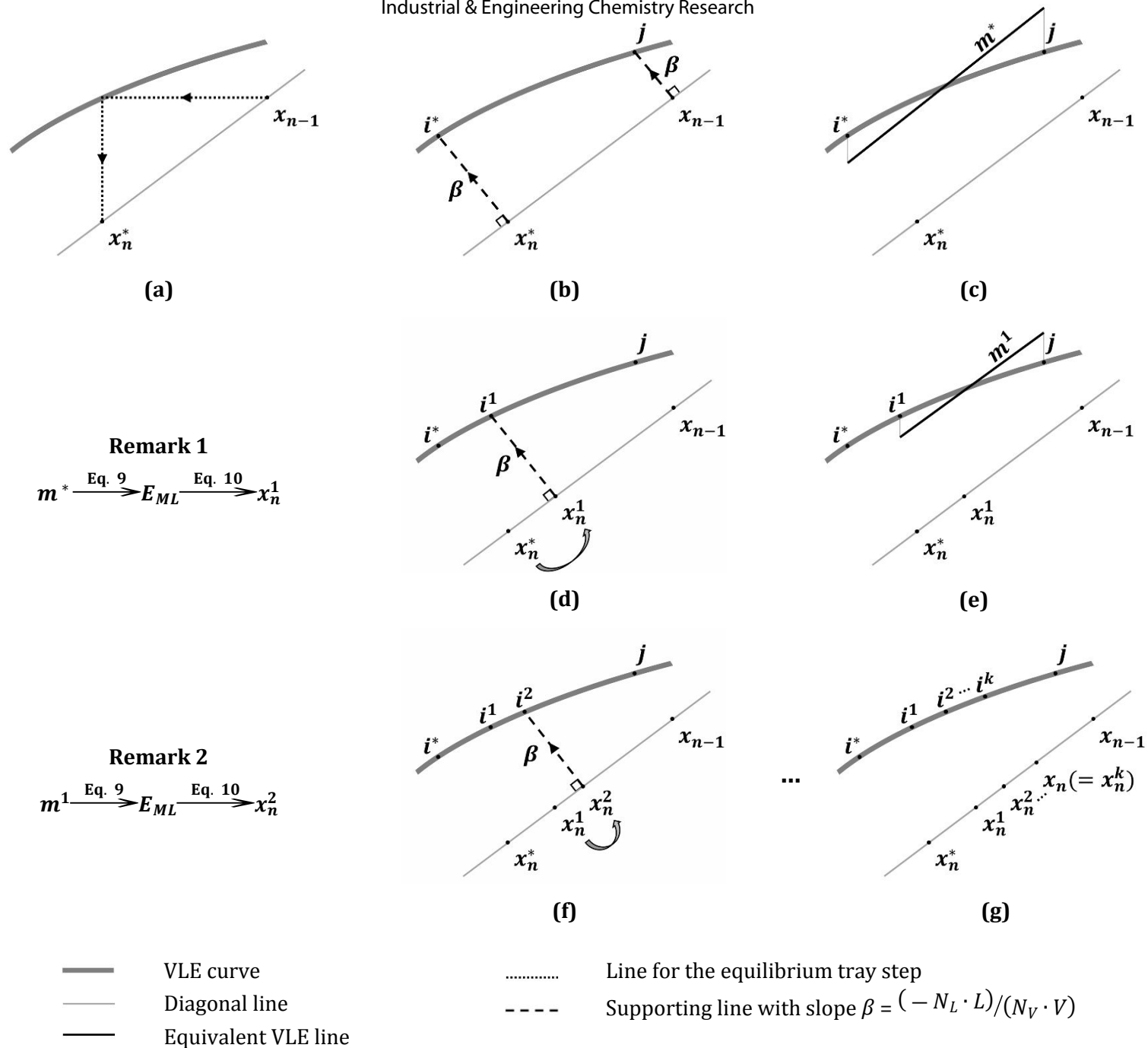
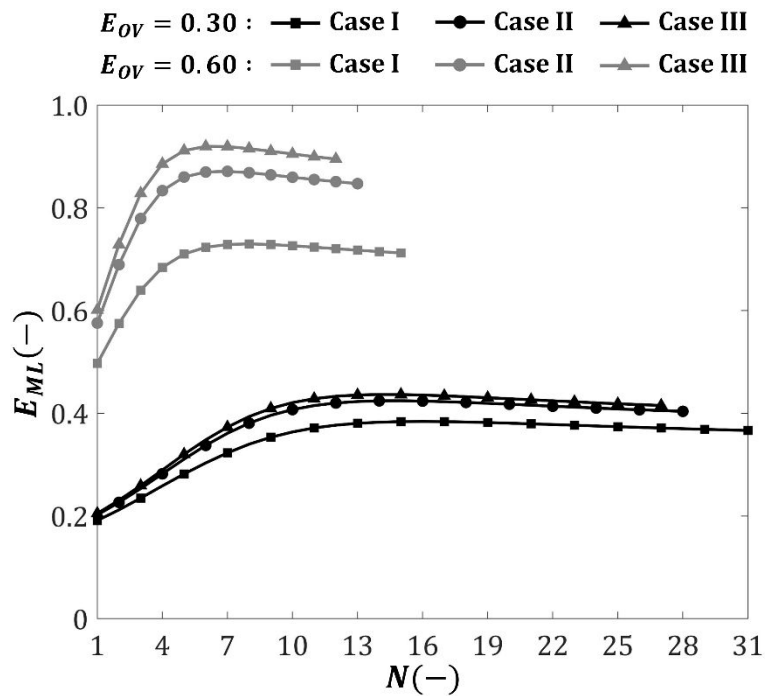


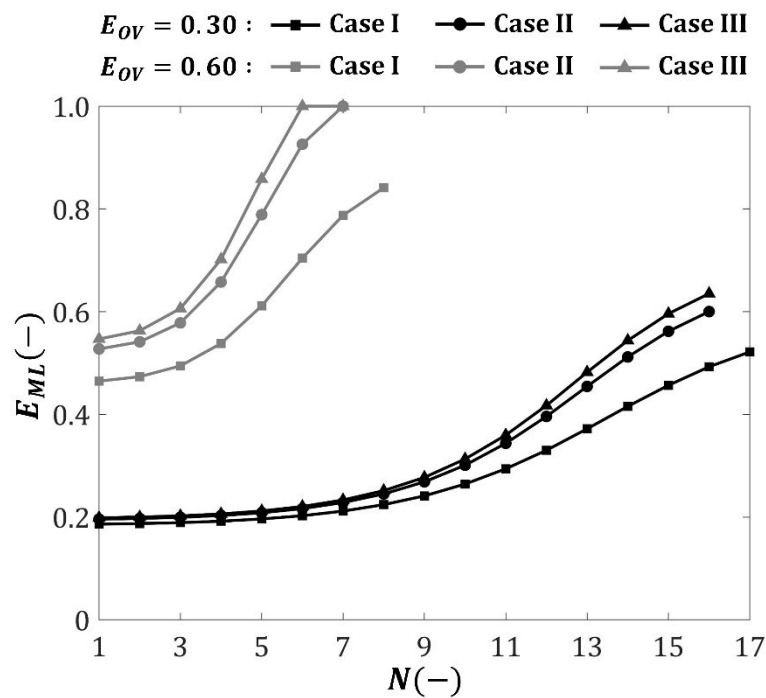
Figure 4. Graphical illustration for estimating the slope of the VLE line (not drawn to scale, figure details and explanations are provided in the text).

2.4 Tray and column efficiency predictions

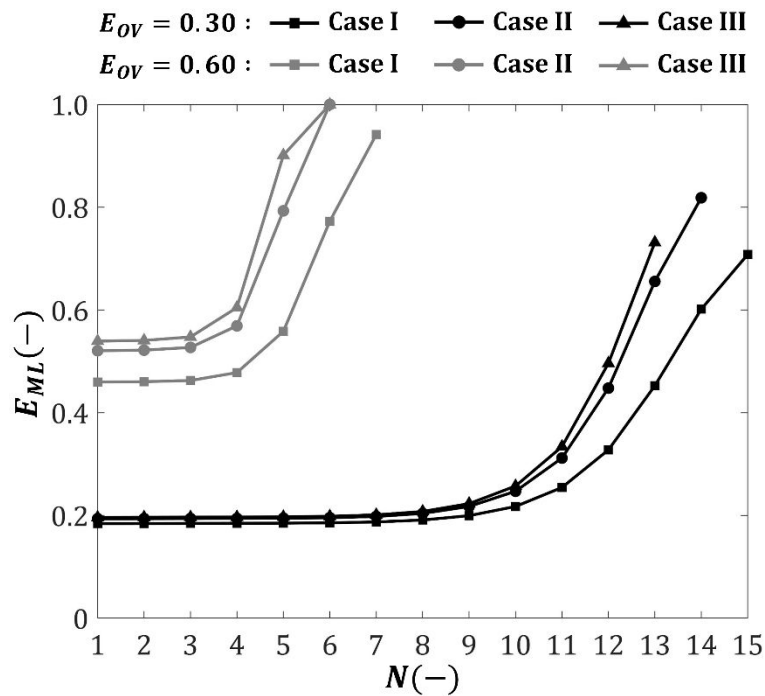
Based on the procedure explained in Section 2.3, the actual number of trays in the column and their efficiencies are calculated for each mixture. The tray efficiency predictions for the three mixtures, whose VLE profiles are shown in Figure 1a, are presented in Figure 5. The predictions for the remaining mixtures listed in Table 1 are provided in Figure S2 in the Supplementary Information. For any given liquid dispersion and point efficiency on the tray, the variation in the tray efficiency (according to eq 9) is caused by the variation of m over the trays in the column (refer to Table S2 in the Supplementary Information). In fact, the variation in m is because of that in the VLE at different temperatures at constant total pressure (see Table S1 in the Supplementary Information). Accordingly, the tray efficiencies vary over the column height for the mixtures for prescribed flow profiles and point efficiencies on the trays. Referring to the x - y plots and efficiency estimates pertaining to the hydrocarbon mixtures in Figures 5, S1 and S2, the difference between the upper and lower limits of m , and hence, the tray efficiency increases with increasing α_{avg} . Hence, using the proposed approach, any variation in the VLE data of a binary mixture can be considered in the column efficiency prediction, since the actual number of trays is known after the tray efficiency calculations. Postulating that m along with flow profiles and point efficiencies remain constant over the trays, then each tray in the column would perform with the same efficiency. This simplification is followed in AIChE's manual using eq 3 for column efficiency predictions,¹³ which is currently the most applied method in the literature. The refined procedure proposed here is clearly superior in this regard.



(a) Water-acetic acid



(b) Benzene-toluene



(c) Methanol-water

Figure 5. Tray efficiency predictions based on VLE data, flow profiles and point efficiencies for selected mixtures. (cases of liquid backmixing: I – severe, II – intermediate, and III – low)

Space left for Figure 6

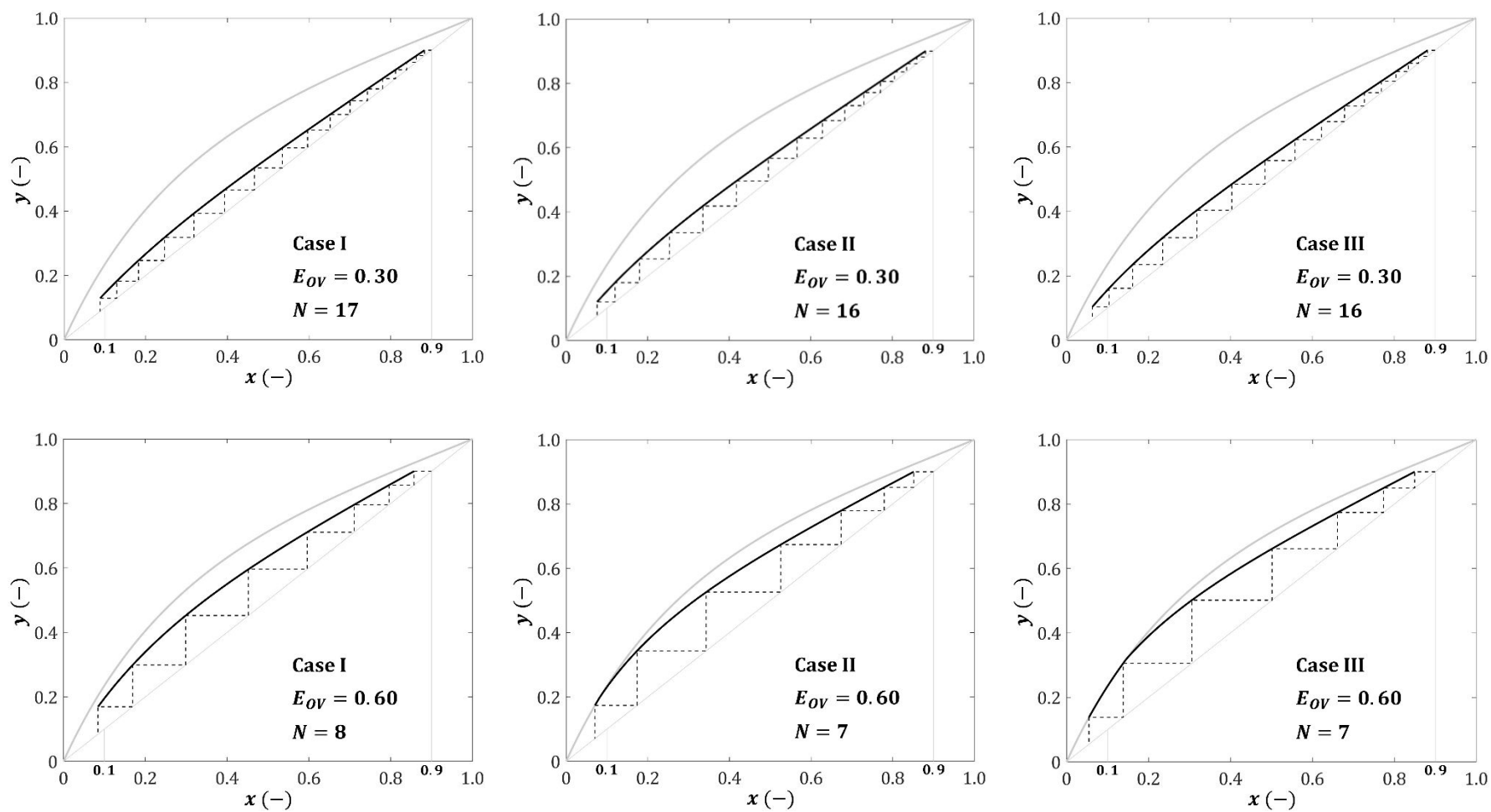


Figure 6. Actual number of trays obtained through efficiency evaluations on the x - y charts for the benzene-toluene mixture. (cases of liquid backmixing: I – severe, II – intermediate, and III – low)

1
2
3 For a constant point efficiency on each tray, the tray efficiency is expectably the lowest in Case I,
4 intermediate in Case II, and the highest in Case III (see Figure 5 earlier and Figure S2 in the
5 Supplementary Information). This happens because the amount of axial liquid mixing associated with
6 each RTD function decreases from Case I to Case III (see Section 2.2). Further, the tray efficiency
7 increases with increasing point efficiencies for given RTD functions and estimated slopes on each tray.
8 Hence, the number of trays actually needed in the column for achieving the targeted separation task is
9 the highest in Case I, intermediate in Case II, and the lowest in Case III at constant point efficiency on
10 each tray. In this scenario, the corresponding number of trays in each case reduces upon the rise in the
11 point efficiency. Moreover, the estimated values of m are fairly high on the lower trays in the column
12 for some mixtures. This can be visualized in the x - y charts shown in Figure S1 in the Supplementary
13 Information. When the higher values of m combine with low axial liquid mixing and high point
14 efficiencies, then the corresponding tray efficiencies becomes greater than unity (not shown here). It is
15 possible for the Murphree tray efficiency to exceed unity especially for large columns and systems of
16 high relative volatilities.^{32,51} In that case, the resulting tray step (as illustrated in Figure 4) would
17 actually transcend the VLE curve. Thus, the maximum tray efficiency is limited to unity here. For
18 example, the efficiencies of the Trays 6 and 7 in the column processing the benzene-toluene mixture in
19 Case III at $E_{OV} = 0.60$ are higher than 100%. Hence, the efficiencies of these trays are restricted to their
20 prescribed limit as shown in Figure 5b. This restriction is also applied to other mixtures. These findings
21 about the tray efficiencies and the resulting number of trays can also be visualized in the x - y charts
22 shown for the benzene-toluene mixture in Figure 6 (x - y charts for the remaining two mixtures
23 considered in Figures 1b and 5 are provided in Figure S3 in the Supplementary Information). The
24 dashed line steps convey the predicted tray efficiencies based on the estimated slopes, considered
25 dispersion numbers and point efficiencies. The black continuous curve depicts the locus of the
26 compositions of liquid and vapor streams exiting the trays for each given condition. This curve is
27 referred to as pseudo-equilibrium curve in the literature.⁵² It can be deduced that the column requires
28
29
30
31
32
33
34
35
36
37
38
39
40
41
42
43
44
45
46
47
48
49
50
51
52
53
54
55
56
57
58
59
60

higher number of (actual) trays, when the pseudo-equilibrium curve shifts towards the diagonal line. On the other hand, lower number of trays are needed in the column, when the pseudo-equilibrium curve shifts towards the VLE curve. Besides, for mixtures with high α_{avg} , the pseudo-equilibrium curve overlaps with a certain range of the VLE curve in the lower part of the column. This can be observed in the Cases II and III at $E_{OV} = 0.60$ in Figures 6e, 6f and S3 in the Supplementary Information. This is because the maximum tray efficiency is limited to unity in this work.

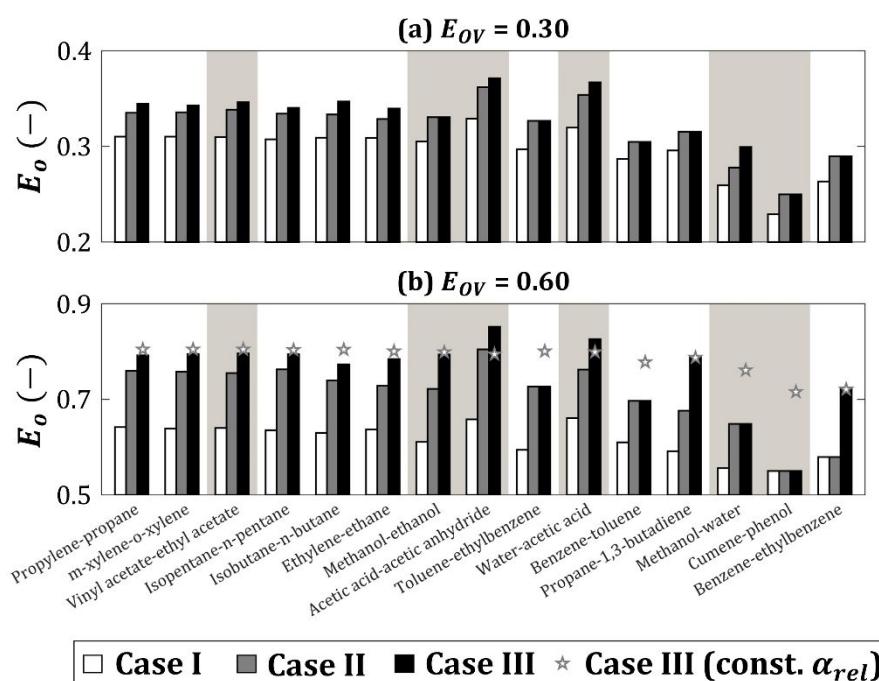


Figure 7. Overall column efficiency predictions for the considered binary mixtures. (cases of liquid backmixing: I – severe, II – intermediate, and III – low)

Figure 7 summarizes the determined overall column efficiency for each mixture depending on given RTD functions, point efficiencies and estimated slopes. Here, the mixtures are arranged on the x -axis in an increasing order of their α_{avg} . In this figure, the predictions with white background correspond to hydrocarbon mixtures, whereas the remaining mixtures are displayed with grey background. As stated

1
2
3 earlier, the column efficiencies are determined here based on fractional number of equilibrium stages,
4 and actual number of trays rounded off to the next integer using eq 1. For any particular point
5 efficiency on the trays, the column efficiency is the lowest in Case I, intermediate in Case II, and the
6 highest in Case III for each mixture. This is because the number of trays needed in the column for the
7 targeted separation task reduces from Case I to Case III owing to the reduction in axial liquid mixing on
8 them (see Figures 5 and S2 in the Supplementary Information). Further, for any particular RTD
9 function, the column efficiency increases with the point efficiency for each mixture. Besides, for some
10 mixtures (especially with high relative volatilities), the column efficiency remains constant in Figure 7
11 irrespective of the liquid dispersion on the trays at a given point efficiency. For example, the overall
12 efficiencies of the column processing benzene-toluene mixture in Cases II and III are the same. This is
13 because the fractional numbers of actual trays for this mixture are 15.5 and 15.1 at $E_{OV} = 0.30$, and 6.7
14 and 6.5 at $E_{OV} = 0.60$, respectively. Rounding off these numbers to the next integer conceals the effect
15 of the flow profiles on the column efficiency in case of mixtures with high α_{avg} . Hence, the fractional
16 number of actual trays for each mixture is provided in Table S3 in the Supplementary Information for
17 the given cases. Furthermore, the trend of efficiency predictions for the given mixtures can be
18 examined via predictions corresponding to the hypothetical mixtures. Therefore, the column efficiency
19 predictions for 15 hypothetical mixtures with constant α over the trays (with the numerical values
20 same as α_{avg} given for the mixtures in Table 1) are presented only for Case III at $E_{OV} = 0.60$ in Figure 7.
21 For hypothetical mixtures, the simulation starts with their VLE data, which is obtained using
22
23
24
25
26
27
28
29
30
31
32
33
34
35
36
37
38
39
40
41
42
43
44

$$y = \frac{\alpha \cdot x}{1 + (\alpha - 1) \cdot x} \quad (11)$$

45
46
47
48
49 Following the procedure discussed in the Sections 2.2 and 2.3, the column efficiencies are estimated by
50 computing N_{min} and N without rounding off. The column efficiencies of these mixtures are nearly
51 uniform until $\alpha = 2$, that approximately corresponds to the toluene-ethylbenzene mixture in Figure 7.
52 For $\alpha \geq 2$, the column efficiencies of the hypothetical mixtures decline as shown in this figure. If the
53
54
55
56
57

fractional values of N are used in eq 1 for the hydrocarbon mixtures, then their column efficiencies are nearly identical to those of the corresponding hypothetical mixtures (not shown here). Of course, this holds for the same dispersion number and point efficiency on the column trays for those mixtures. This happens because α is approximately uniform in case of hydrocarbon mixtures. These observations also hold for other mixtures with low α_{avg} , such as vinyl-acetate-ethyl acetate and methanol-ethanol, since the variation in α is insignificant for those mixtures. However, α varies significantly for other mixtures with higher α_{avg} (such as those given in Figure 1b), where the column efficiencies do not follow the trend of those of the corresponding hypothetical mixtures upon considering fractional values of N in eq 1. For these mixtures, when α values are lower on the top tray than those on the bottom tray, then the column efficiency is also lower than that of the corresponding hypothetical mixture, and vice-versa. For example, the mean values of α for topmost and bottommost trays for acetic acid-acetic anhydride, methanol-water, and cumene-phenol mixtures are approximately 2.8 and 1.0, 2.1 and 5.0, and 2.4 and 8.2, respectively. Thus, with respect to the estimations pertaining to the corresponding hypothetical mixtures in Figure 7, the column efficiency is higher for acetic acid-acetic anhydride mixture, and lower for methanol-water and cumene-phenol mixtures. Further, when the difference between the mean α values on topmost and bottommost trays is high, then the difference between the column efficiency and that of the corresponding hypothetical mixture is also high, and vice-versa. This can be seen for the estimations related to methanol-water and cumene-phenol mixtures in Figure 7. Moreover, binary mixtures with high relative volatilities are easy to separate via distillation, and hence require less number of trays in the column.⁵ However, this is only possible when the column trays operate with low liquid backmixing and high point efficiency. Otherwise, higher number of trays are needed for the separation target, thereby deteriorating the overall column efficiency.

3. Case study II

1
2
3 The application of the proposed procedure for efficiency estimation of an industrial column is
4 attempted in this section. More than a decade ago, Taylor¹⁶ reported the scarcity of the real column
5 data of sufficient quality in the accessible literature that could be used for performance evaluation,
6 which still holds for today. As per authors' knowledge, the only performance data of an operational
7 column that can be used in this work is available in AIChE's reports cited here.^{13,41} The details of the
8 available data followed by efficiency calculations are discussed in the following section.
9
10
11
12
13
14
15
16
17
18

19 **3.1 Background information**

20
21
22 The aforesaid reports provide performance test data of a column operated by Eastman Kodak (New
23 York). A 1.66 m diameter column, containing 60 single-pass bubble-cap trays (labelled from the
24 bottom), was operated in the total reflux mode in three different test runs. In the calculation sheet of
25 AIChE's manual,¹³ the first test run is considered for predicting the column efficiency using eq 3. Hence,
26 the information only pertaining to the first test run is considered here. The mixture of methylene
27 dichloride (CH_2Cl_2) and ethylene dichloride ($\text{C}_2\text{H}_4\text{Cl}_2$) was processed in the column at an average total
28 pressure of 2.34 bar. For this system, 10 VLE (i.e., temperature-mole fraction) data points were
29 provided considering ideal phases of liquid and vapor. Liquid samples were withdrawn from different
30 trays under steady-state conditions. It was found that the Trays 1 to 27 contained almost pure ethylene
31 dichloride, whereas the Trays 35 to 60 had nearly pure methylene dichloride. Technically, these trays
32 were inactive as far as thermal separation is concerned. The data for the inlet liquid composition were
33 given for the Trays 34, 32 and 28 as 99.40%, 95.94% and 18.20%, respectively. According to the
34 recommendation of Górak and Schoenmakers,² extreme component purities are avoided in the present
35 work, and hence, the section involving the Trays 32 to 29 (4 trays) is considered. Further, the tray and
36 point efficiencies were determined experimentally for Tray 32. For this tray, the numerical values
37 given for N_L , N_V , Pe , E_{OV} and E_{MV} are 1.55, 13.0, 27.8, 77.2% and 84.5%, respectively. Further details
38
39
40
41
42
43
44
45
46
47
48
49
50
51
52
53
54
55
56
57
58
59
60

about the column and tray design, plant test data and procedure, and determination of the given parameters can be found in the recommended literature.

Based on the earlier-mentioned decision tree,²⁰ the UNIQUAC model is selected to obtain more reliable and high resolution VLE data for the given system. Applying this model and the provided total pressure in Aspen Plus (v10), 500 VLE data points are generated that can be acquired from the RODARE repository.²³ The reduced VLE data (i.e. with 50 points) for this mixture are also provided in Table S4 in the Supplementary Information. According to eq 4, the average relative volatility over the selected column section is 3.89. Then, using the MT method, N_{min} is obtained as 3.63 as shown in Figure S4 in the Supplementary Information. Substituting the fractional value of N_{min} and the actual number of trays (= 4) in eq 1 determines the actual section efficiency that is 90.75%. This efficiency is used here for evaluating the prediction from the proposed procedure as well as that from eq 3.

3.2 Tray and column efficiency predictions

Following the sequence of steps illustrated in Figure 3, the trays are stepped from bottom to top as originally labelled in the column. Similar to Case study I (see Section 2.3), it is assumed that the given parameters such as phase transfer units (N_L and N_V), point efficiency (E_{OV}), and Péclet number (Pe) for the liquid flow remain same on each tray. Then, the AIChE model is recommended in the mentioned reports for predicting the tray efficiencies based on these given parameters. In the literature,^{3,41} this model is formulated through mass balancing on the two-phase dispersion on a tray as

$$\frac{E_{MV}}{E_{OV}} = \frac{1 - \exp\{-(\eta + Pe)\}}{(\eta + Pe)\left(1 + \frac{\eta + Pe}{\eta}\right)} + \frac{\exp(\eta) - 1}{\eta\left(1 + \frac{\eta}{\eta + Pe}\right)}, \text{ where} \quad (13)$$

$$\eta = \frac{Pe}{2} \left(\sqrt{1 + \frac{4\lambda E_{OV}}{Pe}} - 1 \right) . \quad (14)$$

1
2
3 This model assumes a linear VLE relationship and a constant point efficiency for the tray. Although not
4 explicitly mentioned, plug flow of vapor through the tray with perfect mixing in the disengagement
5 space between the consecutive trays is considered in the model formulation. This model considers
6 liquid backmixing on the tray through Pe , which is referred to as 'simple backmixing model' by Porter
7 et al.⁴² Again, λ reduces to m in the above equation because of the total reflux operation and the linear
8 VLE assumption. Similar to the procedure explained in Section 2.3, m and E_{MV} are estimated using

$$E_{MV} = \frac{y_n - y_{n-1}}{y_n^* - y_{n-1}}, \quad (15)$$

9
10
11
12
13
14
15
16
17
18
19
20
21 and the AIChE model for the lowest tray in the section (i.e., Tray 29 with outlet liquid composition as
22 18.2%). The reader should note, however, that the labeling convention used for the trays in the column
23 is from bottom to top in eq 15, whereas the top-to-bottom approach is considered in eq 10. Further, an
24 operating line is a relationship between the compositions of vapor and liquid entering and leaving the
25 trays in a section, respectively, that is based on the assumption of constant molar overflow.⁵ Therefore,
26 for Tray 29, the outlet liquid composition becomes the inlet vapor composition, because the operating
27 line for this section is the diagonal line. Besides, no correction for the tray efficiency regarding
28 entrainment and weeping was provided in the reports, and hence, it is neglected for all trays here.
29 Eventually, the entire procedure for determining the tray efficiencies in the section is repeated until the
30 stepping procedure reaches to the liquid composition exiting Tray 33 as shown in Figure 8. Moreover,
31 the maximum limit for the tray efficiency is again prescribed as 100% here. The estimated value of m
32 decreases from bottom to top in the column, which gets reflected in the tray efficiency predictions in
33 this figure. The occurrence of low axial liquid mixing, high point efficiency and high values of m on the
34 trays lead to higher tray efficiencies. Therefore, the pseudo-equilibrium curve in Figure 8 (displayed as
35 the black continuous curve) lies in the immediate vicinity of the actual VLE curve (shown as the gray
36 continuous curve). Further, the estimated values of m and E_{MV} for Tray 32 are 0.28 and 85.6%,
37 respectively. This observation validates the AIChE model, since the predicted tray efficiency agrees
38
39
40
41
42
43
44
45
46
47
48
49
50
51
52
53
54
55
56
57
58
59
60

1
2
3 well to that obtained in the performance test run.¹³ Further, these estimations recommend 4 trays in
4 the section for the given composition specifications. Therefore, the proposed procedure estimates the
5 section efficiency that is same as the actual. This agreement also justifies the prescribed limitation of
6 the maximum tray efficiency as unity in this procedure. In fact, the typical values for the tray efficiency
7 range between 50% and 70% according to Cheremisinoff.⁵³ As stated earlier, the information
8 pertaining to Tray 32 were used for predicting the section efficiency in AIChE's manual. Based on those
9 information, the section efficiency according to eq 3 is 75.4%, which is clearly an underestimation. If
10 the manual's approach is explored for the remaining trays, i.e., for Trays 29, 30, and 31, the estimated
11 section efficiencies are 100%, 100% and 83.8%, respectively. Different predictions for the section
12 efficiency are obtained because of the different numerical values of m , and hence, E_{MV} on each tray. The
13 only prediction involving eq 3 that is close to the actual section efficiency is based on the information of
14 Tray 31, which could be fortuitous. Any rule for selecting a particular tray whose conditions are
15 susceptible for an accurate section or column efficiency prediction is unknown and there may not be
16 any such rule in reality. Besides, a deterministic approach is needed for meaningful estimation of the
17 column and section efficiencies that are based on flow profiles and VLE data. Such requirement favors
18 the applicability of the proposed procedure over that employed in AIChE's manual. Simple empirical
19 models (e.g., O'Connell's correlation) are inapplicable for efficiency comparison here, because they
20 require feed liquid viscosity as an input (see eq 2). Indeed, more performance data from industrial
21 columns are needed in the literature for further analyzing the capabilities of the proposed procedure.
22
23
24
25
26
27
28
29
30
31
32
33
34
35
36
37
38
39
40
41
42
43
44
45
46
47
48
49
50
51
52
53
54
55
56
57
58
59
60

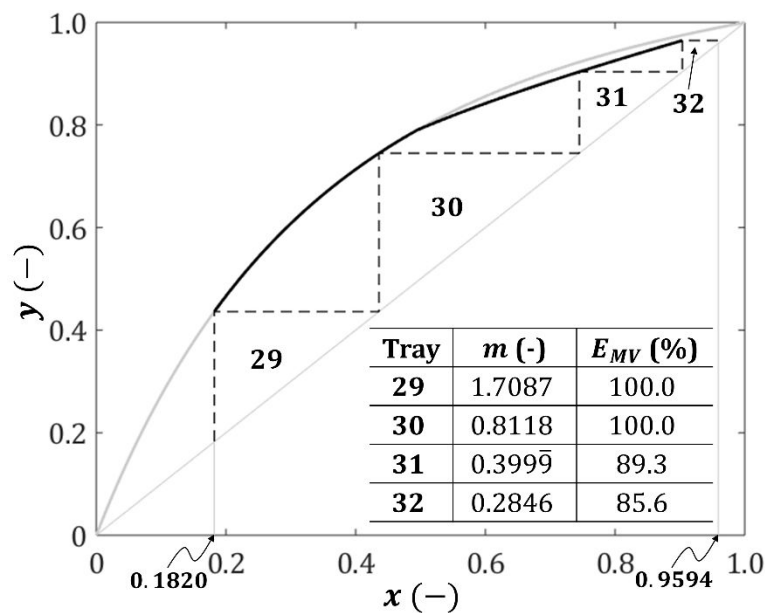


Figure 8. Slope and tray efficiency estimations along with the pseudo-equilibrium curve for the column processing methylene dichloride-ethylene dichloride mixture.

4. Conclusion and future work

A new systematic approach for estimating the column and section efficiencies based on flow profiles on the trays and VLE characteristics of binary mixtures has been proposed in this work. Such an approach would allow a priori estimation of the column performance in the tray and column design phase. This could be advantageous for the industry, as sometimes the potential areas for improving tray and column performances become known after the design phase leading to considerable losses in terms of cost and energy. A key feature of the proposed approach is the approximation of the slope of the VLE curve and the Murphree tray efficiency using an iterative technique. The capabilities of the new approach are demonstrated in two case studies, where the impact of point efficiencies, flow distributions and VLE data on the column efficiencies are presented. These information have not been considered exclusively for each tray by the existing approaches pertaining to column efficiency

1
2
3 estimation. A detailed analysis of the case studies confirms the superiority of the new approach over
4
5 the most applied method in the literature.
6

7
8 In the future, an advanced tray efficiency prediction model²⁵ capable of considering vapor
9
10 maldistribution on the trays could be considered in the proposed approach. Such an inclusion is
11
12 expected to refine the predictive capabilities of this approach. Additionally, if pressure variations over
13
14 the column height are known, then their impact on the tray column performance can also be
15
16 investigated using the new approach.
17
18
19
20
21

22 **Supporting Information Available**

23
24
25 VLE data for binary mixtures obtained from various thermodynamic models at representative column
26
27 pressures in Case Study I; Estimation of slope of the VLE curve in Case Study I (approach 1: line fitting,
28
29 approach 2: slope averaging); Fractional number of actual trays for each mixture in Case Study I; VLE
30
31 data of methylene dichloride-ethylene dichloride mixture in Case Study II; Minimum number of stages
32
33 for each mixture (in the ascending order of α_{rel}) using the McCabe-Thiele method; Tray efficiency
34
35 predictions for binary mixtures based on prescribed flow profiles and point efficiencies. (cases of liquid
36
37 backmixing: I – severe, II – intermediate, and III – low); Actual number of trays obtained through
38
39 efficiency evaluations on the x - y charts for (a) water-acetic acid, and (b) methanol-water mixtures.
40
41 (cases of liquid backmixing: I – severe, II – intermediate, and III – low); Minimum number of stages in
42
43 Case study II (methylene dichloride-ethylene dichloride, $P = 2.34$ bara, $N_{min} = 3.63$) based on McCabe-
44
45 Thiele method.
46
47
48
49
50
51
52
53
54
55
56
57
58
59
60

AUTHOR INFORMATION

Corresponding Authors

*Tel.: +49 351 260 3778. Fax: +49 351 260 2383. E-mail: v.vishwakarma@hzdr.de

*Tel.: Tel.: +49 351 260 2627. Fax: +49 351 260 2383. E-mail: m.schubert@hzdr.de

ORCID

Vineet Vishwakarma: 0000-0002-5428-4112

Markus Schubert: 0000-0002-6218-0989

Notes

The authors declare no competing financial interest.

Acknowledgment

The first author (V.V.) gratefully acknowledges the financial support from German Academic Exchange Service (Deutscher Akademischer Austauschdienst, DAAD; grant number 91563198). The second author (N.R.) acknowledges the financial support from Erasmus+ programme (grant number 2115). We are thankful to Dr. Epaminondas Voutsas (School of Chemical Engineering, National Technical University of Athens, Greece) for his input on the proper selection of thermodynamic models for the VLE data of binary mixtures.

Nomenclature

D_E Eddy diffusion coefficient (m^2/s)

E_{ML} Murphree liquid-phase tray efficiency (-)

1		
2		
3	E'_{ML}	Murphree liquid-phase tray efficiency corrected for entrainment and weeping (-)
4		
5		
6	E_{MV}	Murphree vapor-phase tray efficiency (-)
7		
8		
9	E_{OV}	Murphree vapor-phase point efficiency (-)
10		
11	E_o	Section or overall column efficiency (-)
12		
13		
14	$f(t)$	Residence time distribution function (s^{-1})
15		
16		
17	i, j	Intersection of supporting lines with the VLE curve (-)
18		
19	k	Iteration index in the slope calculation (-)
20		
21		
22	L	Liquid flow rate (mol/s)
23		
24		
25	m	Slope of the VLE line (-)
26		
27	N	Actual number of trays (-)
28		
29		
30	N_{eq}	Number of equilibrium stages (-)
31		
32		
33	N_L	Number of binary liquid-phase transfer units (-)
34		
35		
36	N_{min}	Minimum number of trays (-)
37		
38	N_{OV}	Number of overall binary vapor-phase transfer units (-)
39		
40		
41	N_{TD}	Tray dispersion number (-)
42		
43		
44	N_V	Number of binary vapor-phase transfer units (-)
45		
46		
47	P	Total pressure (bar)
48		
49	Pe	Péclet number (-)
50		
51		
52	t	Time (s)
53		
54		
55	V	Vapor or gas flow rate (mol/s)
56		
57		

1		
2		
3	x	Composition (mole fraction) of the volatile component in the liquid phase (-)
4		
5		
6	x_n	Composition of the liquid stream exiting the n^{th} tray (-)
7		
8		
9	x_n^*	Liquid composition that is in equilibrium with the vapor exiting the n^{th} tray (-)
10		
11		
12	x_{n-1}	Composition of the liquid stream entering the n^{th} tray (-)
13		
14		
15	y_n	Composition of the vapor stream exiting the n^{th} tray (-)
16		
17		
18	y_n^*	Vapor composition that is in equilibrium with the liquid exiting the n^{th} tray (-)
19		
20		
21	y_{n-1}	Composition of the vapor stream entering the n^{th} tray (-)
22		
23		
24	y	Composition (mole fraction) of the volatile component in the vapor phase (-)
25		
26	Z	Flow path length (m)
27		
28		
29		
30		

Greek Letters

31		
32		
33		
34	α	Relative volatility (-)
35		
36		
37	β	Slope of the supporting line in Figure 4 (-)
38		
39		
40	δ	Dirac delta function (s^{-1})
41		
42	λ	Stripping factor ($= mV/L$) (-)
43		
44		
45	μ_L	Average liquid viscosity of the feed (mPa-s)
46		
47		
48	τ	Mean residence time of liquid on a tray (s)
49		
50		
51	τ_h	Hydraulic or space time (s)
52		
53		
54		
55		

Subscripts

1		
2		
3	<i>avg</i>	Average
4		
5		
6	<i>B</i>	Bottom stream
7		
8	<i>L</i>	Liquid
9		
10		
11	<i>n</i>	n^{th} tray
12		
13		
14	<i>T</i>	Top stream
15		
16	<i>V</i>	Vapor or gas
17		
18		
19		
20		
21		

Abbreviations

22		
23		
24	<i>ADM</i>	Axial dispersion model
25		
26		
27	<i>AIChE</i>	American Institute of Chemical Engineers
28		
29		
30	<i>MT</i>	McCabe-Thiele
31		
32		
33	<i>RTD</i>	Residence time distribution
34		
35	<i>VLE</i>	Vapor-liquid equilibrium
36		
37		
38		
39		

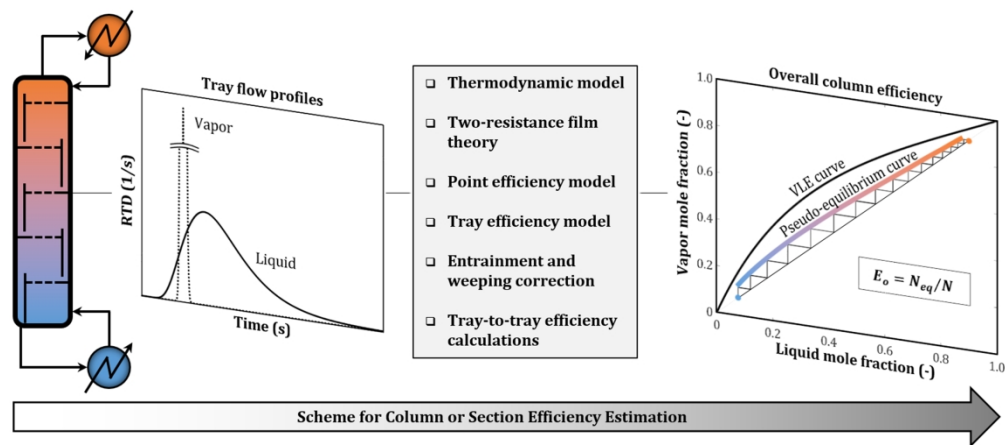
References

1. Lockett MJ. *Distillation tray fundamentals*. Cambridge University Press; **1986**.
2. Gorak A, Schoenmakers H. *Distillation: operation and applications*. Academic Press; **2014**.
3. Vishwakarma V, Schubert M, Hampel U. Assessment of separation efficiency modeling and visualization approaches pertaining to flow and mixing patterns on distillation trays. *Chem Eng Sci*. **2018**;185:182-208.
4. Sholl DS, Lively RP. Seven chemical separations to change the world. *Nature News*. **2016**;532(7600):435.
5. Górak A, Sorensen E. *Distillation: fundamentals and principles*. Academic Press; **2014**.
6. Górak A, Olujic Z. *Distillation: equipment and processes*. Academic Press; **2014**.

- 1
- 2
- 3 7. Luo N, Qian F, Ye Z-C, Cheng H, Zhong W-M. Estimation of mass-transfer efficiency for industrial
- 4 distillation columns. *Ind Eng Chem Res.* **2012**;51(7):3023-3031.
- 5
- 6 8. Nielsen RF, Huusom JK, Abildskov J. Driving force based design of cyclic distillation. *Ind Eng*
- 7 *Chem Res.* **2017**;56(38):10833-10844.
- 8
- 9 9. McCabe WL, Thiele E. Graphical design of fractionating columns. *Ind Eng Chem.*
- 10 **1925**;17(6):605-611.
- 11
- 12 10. O'connell H. Plate efficiency of fractionating columns and absorbers. *Trans AIChE.*
- 13 **1946**;42:741-755.
- 14
- 15
- 16 11. Duss M, Taylor R. Predict distillation tray efficiency. *Chem Eng Prog.* **2018**;114(7):24-30.
- 17
- 18 12. Lewis Jr WK. Rectification of binary mixtures. *Ind Eng Chem.* **1936**;28(4):399-402.
- 19
- 20 13. Committee AIoCER. *Bubble-tray design manual prediction of fractionation efficiency.* American
- 21 Institute of Chemical Engineers; **1958**.
- 22
- 23 14. Mathias PM. Visualizing the McCabe-Thiele diagram. *Chem Eng Prog.* **2009**;105(12):36-44.
- 24
- 25 15. Schultes M. Research on mass transfer columns: passé? *Chem Eng Technol.* **2013**;36(9):1539-
- 26 1549.
- 27
- 28 16. Taylor R. (Di) Still modeling after all these years: a view of the state of the art. *Ind Eng Chem*
- 29 *Res.* **2007**;46(13):4349-4357.
- 30
- 31 17. Yanagi T, Sakata M. Performance of a commercial scale 14% hole area sieve tray. *Ind Eng Chem*
- 32 *Process Des Dev.* **1982**;21(4):712-717.
- 33
- 34 18. Kister HZ. Effects of design on tray efficiency in commercial towers. *Chem Eng Prog.*
- 35 **2008**;104(6):39-47.
- 36
- 37 19. Seader JD, Henley EJ, Roper DK. *Separation process principles.* **1998**.
- 38
- 39 20. De Hemptinne J-C, Ledanois J-M. *Select thermodynamic models for process simulation: A*
- 40 *practical guide using a three steps methodology.* Editions Technip; **2012**.
- 41
- 42 21. Chang W, Guan G, Li X, Yao H. Isobaric vapor- liquid equilibria for water+ acetic acid+(n-pentyl
- 43 acetate or isopropyl acetate). *J Chem Eng Data.* **2005**;50(4):1129-1133.
- 44
- 45 22. Hartono A, Kim I. Calculation of vapor-liquid equilibria for methanol-water mixture using
- 46 cubic-plus-association equation of state. *Project work in the subject KP8108 Adv Thermo.* **2004**.
- 47
- 48 23. Vishwakarma V, Rigos N, Schubert M, Hampel U. Vapor-liquid equilibrium data for efficiency
- 49 estimation of tray columns [Data set]. In: Rodare, ed**2019**.
- 50
- 51 24. Sahai Y, Emi T. Melt flow characterization in continuous casting tundishes. *ISIJ Int.*
- 52 **1996**;36(6):667-672.
- 53
- 54 25. Vishwakarma V, Schubert M, Hampel U. Development of a refined RTD-based efficiency
- 55 prediction model for cross-flow trays. *Ind Eng Chem Res.* **2019**;58(8):3258-3268.
- 56
- 57
- 58
- 59
- 60

- 1
- 2
- 3 26. Vishwakarma V, Schubert M, Hampel U. A novel RTD compartment model for tray efficiency
- 4 predictions. *Chem Eng Trans.* **2018**;69:331-336.
- 5
- 6 27. Nauman EB. Residence time theory. *Ind Eng Chem Res.* **2008**;47(10):3752-3766.
- 7
- 8 28. Levenspiel O. *Chemical reaction engineering.* 3rd ed: John Wiley and Sons; **1999**.
- 9
- 10 29. Fogler HS, Gürmen MN. *Elements of chemical reaction engineering (online version).* 4th ed:
- 11 University of Michigan; **2008**.
- 12
- 13 30. Shah Y, Stiegel G, Sharma M. Backmixing in gas-liquid reactors. *AIChE J.* **1978**;24(3):369-400.
- 14
- 15 31. Abu-Reesh IM, Abu-Sharkh BF. Comparison of axial dispersion and tanks-in-series models for
- 16 simulating the performance of enzyme reactors. *Ind Eng Chem Res.* **2003**;42(22):5495-5505.
- 17
- 18 32. Kister HZ, Haas JR, Hart DR, Gill DR. *Distillation design.* Vol 1: McGraw-Hill New York; **1992**.
- 19
- 20 33. Chen GX, Chuang KT. Liquid-phase resistance to mass transfer on distillation trays. *Ind Eng*
- 21 *Chem Res.* **1995**;34(9):3078-3082.
- 22
- 23 34. Chen GX, Chuang KT. Determining the number of gas-phase and liquid-phase transfer units
- 24 from point efficiencies in distillation. *Ind Eng Chem Res.* **1994**;33(4):907-913.
- 25
- 26 35. Lockett M, Plaka T. Effect of non-uniform bubbles in the froth on the correlation and prediction
- 27 of point efficiencies. *Chem Eng Res Des.* **1983**;61:119-124.
- 28
- 29 36. Moens F, Bos R. Surface renewal effects in distillation. *Chem Eng Sci.* **1972**;27(2):403-408.
- 30
- 31 37. Zuiderweg F. Sieve trays: a view on the state of the art. *Chem Eng Sci.* **1982**;37(10):1441-1464.
- 32
- 33 38. Stichlmair J, Ulbrich S. Liquid channelling on trays and its effect on plate efficiency. *Chem Eng*
- 34 *Technol.* **1987**;10(1):33-37.
- 35
- 36 39. Gautreaux MF, O'Connell HE. Effect of length of liquid path on plate efficiency. *Chem Eng Prog.*
- 37 **1955**;51(5):232-237.
- 38
- 39 40. Bruin S, Freije A. A simple liquid mixing model for distillation plates with stagnant zones. *Trans*
- 40 *Inst Chem Eng.* **1974**;52(1):75-79.
- 41
- 42 41. Gerster J, Hill A, Hochgraf N, Robinson D. *Tray efficiencies in distillation columns final report.*
- 43 Univ. of Delaware, Newark; **1958**.
- 44
- 45 42. Porter KE, Lockett MJ, Lim CT. The effect of liquid channeling on distillation plate efficiency.
- 46 *Trans Inst Chem Eng.* **1972**;50(2):91-101.
- 47
- 48 43. Lockett MJ, Safekourdi A. The effect of the liquid flow pattern on distillation plate efficiency.
- 49 *Chem Eng J.* **1976**;11(2):111-121.
- 50
- 51 44. Bell RL, Solari RB. Effect of nonuniform velocity fields and retrograde flow on distillation tray
- 52 efficiency. *AIChE J.* **1974**;20(4):688-695.
- 53
- 54 45. Foss AS, Gerster JA, Pigford RL. Effect of liquid mixing on the performance of bubble trays.
- 55 *AIChE J.* **1958**;4(2):231-239.
- 56
- 57
- 58
- 59
- 60

- 1
2
3 46. Foss AS. *Liquid mixing on bubble trays and its effect upon plate efficiency* [Doctoral dissertation],
4 Univ. of Delaware; **1957**.
5
6 47. Gao X, Li X, Liu X, Li H, Yang Z, Zhang J. A novel potential application of SiC ceramic foam
7 material to distillation: foam monolithic tray. *Chem Eng Sci*. **2015**;135:489-500.
8
9 48. Li H, Fu L, Li X, Gao X. Mechanism and analytical models for the gas distribution on the SiC foam
10 monolithic tray. *AlChE J*. **2015**;61(12):4509-4516.
11
12 49. Li X, Yan P, Zhao S, Li H, Gao X. Fabrication and hydrodynamics performance of modified sieve
13 tray with Janus feature. *Sep Purif Technol*. **2019**;216:74-82.
14
15 50. Yan P, Li X, Li H, Shao Y, Zhang H, Gao X. Hydrodynamics and mechanism of hydrophobic foam
16 column tray: Contact angle hysteresis effect. *AlChE J*. **2019**.
17
18 51. Onda K, Sada E, Takahashi K, Mukhtar S. Plate and column efficiencies of continuous rectifying
19 columns for binary mixtures. *AlChE J*. **1971**;17(5):1141-1152.
20
21 52. Khoa T, Shuhaimi M, Hashim H, Panjeshahi M. Optimal design of distillation column using three
22 dimensional exergy analysis curves. *Energy*. **2010**;35(12):5309-5319.
23
24 53. Chermisinoff NP. *Handbook of chemical processing equipment*. Elsevier; **2000**.
25
26
27
28
29
30
31
32
33
34
35
36
37
38
39
40
41
42
43
44
45
46
47
48
49
50
51
52
53
54
55
56
57
58
59
60



TOC graphic

338x150mm (300 x 300 DPI)